

University of Nebraska - Lincoln

DigitalCommons@University of Nebraska - Lincoln

Ralph Skomski Publications

Research Papers in Physics and Astronomy

7-2013

Hf Doping Effect on Hard Magnetism of Nanocrystalline Zr_{18-x}Hf_xCo₈₂ Ribbons

Imaddin Ali Al-Omari

Sultan Qaboos University, ialomari@squ.edu.om

Wenyong Zhang

University of Nebraska-Lincoln, wenyong.zhang@unl.edu

Lanping Yue

University of Nebraska-Lincoln, lyue2@unl.edu

Ralph Skomski

University of Nebraska-Lincoln, rskomski2@unl.edu

Jeffrey E. Shield

University of Nebraska-Lincoln, jshield@unl.edu

See next page for additional authors

Follow this and additional works at: <https://digitalcommons.unl.edu/physicsskomski>

Al-Omari, Imaddin Ali; Zhang, Wenyong; Yue, Lanping; Skomski, Ralph; Shield, Jeffrey E.; Li, Xingzhong; and Sellmyer, David J., "Hf Doping Effect on Hard Magnetism of Nanocrystalline Zr_{18-x}Hf_xCo₈₂ Ribbons" (2013). *Ralph Skomski Publications*. 75.

<https://digitalcommons.unl.edu/physicsskomski/75>

This Article is brought to you for free and open access by the Research Papers in Physics and Astronomy at DigitalCommons@University of Nebraska - Lincoln. It has been accepted for inclusion in Ralph Skomski Publications by an authorized administrator of DigitalCommons@University of Nebraska - Lincoln.

Authors

Imaddin Ali Al-Omari, Wenyong Zhang, Lanping Yue, Ralph Skomski, Jeffrey E. Shield, Xingzhong Li, and David J. Sellmyer

Hf Doping Effect on Hard Magnetism of Nanocrystalline $\text{Zr}_{18-x}\text{Hf}_x\text{Co}_{82}$ Ribbons

I. A. Al-Omari^{1,2,3}, W. Y. Zhang^{2,3}, Lanping Yue³, R. Skomski^{2,3}, J. E. Shield^{3,4}, X. Z. Li³, and D. J. Sellmyer^{2,3}

¹Department of Physics, Sultan Qaboos University, Muscat, PC 123, Sultanate of Oman

²Department of Physics and Astronomy, University of Nebraska, Lincoln, NE 68588 USA

³Nebraska Center for Materials and Nanoscience, University of Nebraska, Lincoln, NE 68588 USA

⁴Department of Mechanical and Materials Engineering, University of Nebraska, Lincoln, NE 68588 USA

The effects of substituting Zr by Hf on the structural and the magnetic properties of the nanocrystalline rapidly solidified $\text{Zr}_{18-x}\text{Hf}_x\text{Co}_{82}$ ribbons ($x = 0, 2, 4$, and 6) have been studied. X-ray diffraction and thermomagnetic measurement results indicated that upon rapid solidification processing four magnetic phases occur: rhombohedral $\text{Zr}_2\text{Co}_{11}$, orthorhombic $\text{Zr}_2\text{Co}_{11}$, hcp Co, and cubic $\text{Zr}_6\text{Co}_{23}$ phases. Microstructure analysis results showed the reduction in the percentage of the soft-magnetic phase (Co) compared to the hard-magnetic phase ($\text{Zr}_2\text{Co}_{11}$ (rhombohedral)) with the increase in the Hf concentration. All the samples under investigation have ferromagnetic nature, at 4.2 K and at room temperature. The coercive force (H_c) and the saturation magnetization (M_s) are found to linearly increase with x ($x \leq 2$), then H_c slightly increases and M_s slightly decreases with increasing x . The maximum energy product $(BH)_{\max}$ at room temperature is found to increase with increasing x reaching a maximum value for $x = 4$. The magnetocrystalline anisotropy parameter of these samples are calculated to be $K = 1.1 \text{ MJ/m}^3$ and independent of Hf concentration. The above results indicate that the replacement of Zr by Hf improves the hard-magnetic properties of this class of rare-earth-free nanocrystalline permanent magnet materials.

Index Terms—Energy, magnetization, microstructure, nanomaterials, permanent magnets.

I. INTRODUCTION

INTERMETALLIC compounds of Zr-Co are a fascinating group of materials, which have recently attracted much attention from the viewpoint of fundamentals as well as application. The structural and magnetic properties of the intermetallic Zr-Co alloys depend on the Zr concentration. The hard-magnetic compounds of $\text{Zr}_{18}\text{Co}_{82}$ have a maximum coercive force of 2.7 kOe for nanocrystalline samples and it was found that the magnetic polarization of this alloy can be increased to 11.6 kG after the introduction of 15 at% Fe [1]. This class of materials with the ordered phase at elevated temperatures have promising magnetic properties both in the microcrystalline and nanocrystalline states. Ternary element additions to these systems (such as B, Mo, Si, Al, Fe, Ni) have been used to improve the magnetic and other physical properties [2]–[12].

At present, numerous experimental data are available on the ordered Zr-Co alloy systems, because of their high temperature magnetic properties, excellent oxidation and corrosion resistance. Substitution of Co by other elements affects the magnetic properties, the lattice parameter, and the structural ordering of these alloys. Saito [2] studied the $\text{Co}_{80}\text{Zr}_{20-x}\text{B}_x$ ($x = 0-4$) system and found the existence of three phases, Co_5Zr , $\text{Co}_{23}\text{Zr}_6$, and fcc-Co phase. He also found that the metastable Co_5Zr phase is the one responsible for the hard-magnetic properties of these alloys. The effects of Mo substitution on the

magnetic properties of $\text{Zr}_{18}\text{Co}_{82-x}\text{Mo}_x$ ($x = 1-5$) were studied by Zhang *et al.* [4]. They found that for $x = 5$, a single Co_5Zr phase can be formed with a coercive force of 4.1 kOe and Curie temperature of 450°C, while for $x < 5$, the fcc Co phase exists in addition to the Co_5Zr phase. They also found that upon annealing of the $\text{Zr}_{18}\text{Co}_{77}\text{Mo}_5$ melt-spun ribbons the coercive force decreases to 1.8–2.8 kOe, depending on the annealing temperature. Our recent study on the structure and magnetism of nanocrystalline ribbons of $\text{Zr}_{16}\text{Co}_{78-x}\text{Mo}_x\text{Si}_3\text{B}_3$ ($x = 0-5$) showed that the substitution of Mo for Co restrains the formation of Co, raises the content of $\text{Zr}_2\text{Co}_{11}$, and increases the mean grain size of $\text{Zr}_2\text{Co}_{11}$ [11]. We have shown that the addition of Mo increases the coercivity from 4 kOe for $x = 0$ to 7.9 kOe for $x = 5$ while the saturation magnetization decreases from 7.2 to 3.6 kG for the same compositions. As a result of the decrease in the saturation magnetization, the maximum energy product $(BH)_{\max}$ at room temperature is found to decrease almost from 2.7 MGOe for $x = 0$ to 0.5 MGOe for $x = 5$.

Most of the work done by the different research groups concentrated either on the ratio of Co to Zr or on substituting Co by other elements. While few papers were done on substituting Zr by other elements. It was reported that Hf-Co nanomaterials have good intrinsic and extrinsic properties [13], [14]. Hf is in the VIB group elements like Zr in the periodic table of elements, and has the nearly same atomic radius as Zr. It is expected that there are some positive effects of Hf substitution on magnetic properties of nanocrystalline Zr-Co. In this paper we focused our attention on the preparation of the rapidly solidified $\text{Zr}_{18-x}\text{Hf}_x\text{Co}_{82}$ ribbons for four different samples which allows us to investigate the effects of substituting zirconium by hafnium on the structural and magnetic properties of the $\text{Zr}_{18-x}\text{Hf}_x\text{Co}_{82}$ ribbons.

Manuscript received November 05, 2012; revised January 29, 2013; accepted January 31, 2013. Date of current version July 15, 2013. Corresponding author: I. A. Al-Omari (e-mail: ialomari@squ.edu.om, ialomari@yahoo.com).

Color versions of one or more of the figures in this paper are available online at <http://ieeexplore.ieee.org>.

Digital Object Identifier 10.1109/TMAG.2013.2245498

II. EXPERIMENTAL METHODS

Polycrystalline rapidly solidified $\text{Zr}_{18-x}\text{Hf}_x\text{Co}_{82}$ ribbons ($x = 0, 2, 4$, and 6) were prepared by arc-melting followed by vacuum melt spinning using a rotating copper wheel with a wheel speed of 40 m/s . The structure and phase components of the ribbons were investigated by Rigaku D/Max-B X-ray diffraction (XRD) with $\text{Co K}\alpha$ radiation and JEOL JEM 201 Transmission Electron Microscopy (TEM). The magnetic measurements were carried out at the temperatures of 4.2 and 300 K using a Superconducting Quantum Interference Device (SQUID) magnetometer at fields up to 7 T and a PPMS Vibrating Sample magnetometer (VSM) in the temperature range between 300 and 900 K . Samples were mounted in the sample holder such that the applied field is parallel to the length direction of ribbon. The law of the approach to saturation was used to fit the high-field part of hysteresis loops and estimate the magnetocrystalline anisotropy parameter K [15].

III. RESULTS AND DISCUSSION

Fig. 1(a) shows the x-ray diffraction pattern for the nanocrystalline ribbons system $\text{Zr}_{18-x}\text{Hf}_x\text{Co}_{82}$ ($x = 0, 4$), after converting the wavelength of the Co -radiation to the wavelength of the Cu -radiation. The observed reflection lines obtained at room temperature for all investigated samples exhibit lines characteristic of 4-structures: rhombohedral $\text{Zr}_2\text{Co}_{11}$, orthorhombic $\text{Zr}_2\text{Co}_{11}$, cubic $\text{Zr}_6\text{Co}_{23}$, and hcp Co phases. Fig. 1(b) presents the enlarged part with the separated peaks by the Gaussian fit. The relative intensity of diffraction peak of Co decreases with x , indicating the volume fraction of Co decreases with x , which was also verified by thermomagnetic measurement results. It was concluded that Hf addition favors the formation of rhombohedral $\text{Zr}_2\text{Co}_{11}$. The full-width at half-maximum (FWHM) of the diffraction peak of rhombohedral $\text{Zr}_2\text{Co}_{11}$ is almost constant with the increase of x , which means that the mean grain size of hard phase is unchanged. The FWHM of diffraction peak of Co increases from 0.37 degree for $x = 0$ to 0.50 degree for $x = 4$. This implies that the average grain size of Co decreases with increasing x . Hf addition decreases the grain size of Co .

Fig. 2 shows two representative hysteresis loops for nanocrystalline ribbons system $\text{Zr}_{18-x}\text{Hf}_x\text{Co}_{82}$ with $x = 0$ and $x = 4$. It is clear from these single-hysteresis loops that the hard-magnetic phase and the soft-magnetic phase are strongly exchange-coupled, as shown in the inset of Fig. 2. The saturation magnetization at room temperature is found to increase from 74 emu/g with increasing the Hf concentration (x) reaching a maximum of 76 emu/g at $x = 2$, then it decreases with increasing x reaching 64 emu/g for $x = 6$, while the coercive force is found to increase with increasing x from 2.4 kOe for the parent alloy to 3.3 kOe for $x = 6$, as can be seen from Fig. 3. The increase in the coercive force and the decrease in the saturation magnetization for large x concentrations were attributed to the refinement in the grain size and the decrease in the percentage of the soft-magnetic Co -phase compared to the hard-magnetic $\text{Zr}_2\text{Co}_{11}$ -phase. The saturation magnetization and the coercive force are found to increase with decreasing the temperature from 300 K to 4.2 K , as a result of this increase

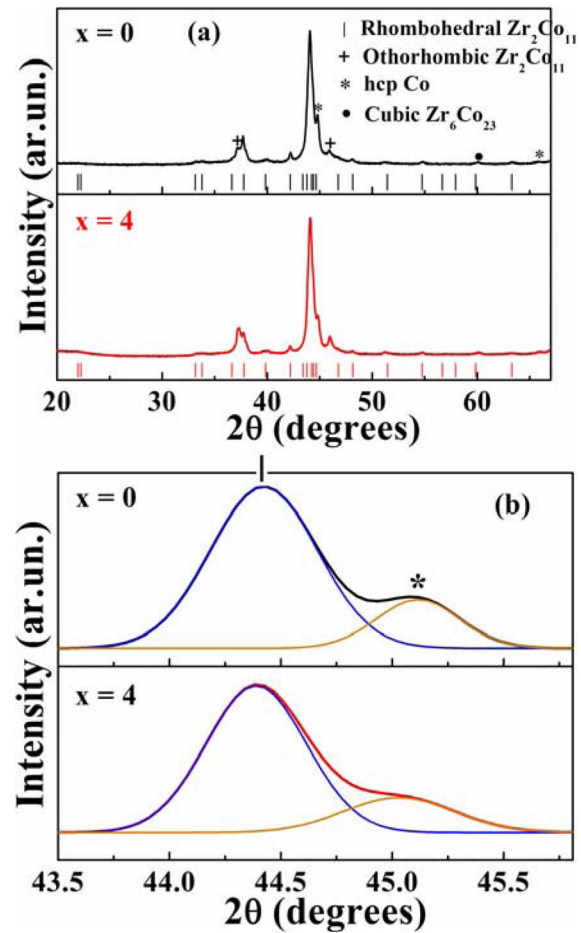


Fig. 1. X-ray diffraction patterns for the nanocrystalline ribbons system $\text{Zr}_{18-x}\text{Hf}_x\text{Co}_{82}$ ($x = 0, 4$) (a) and enlarged part with the peaks separated by Gaussian fit (b).

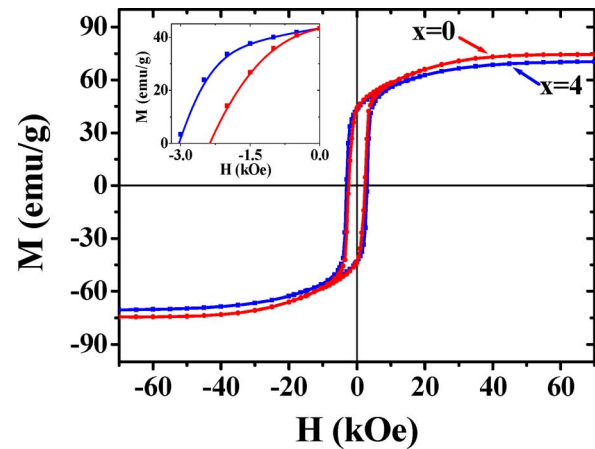


Fig. 2. Room temperature hysteresis loops for two representative samples of the nanocrystalline ribbons system $\text{Zr}_{18-x}\text{Hf}_x\text{Co}_{82}$ ($x = 0$ and 4). The inset represents the enlarged demagnetization curves.

the maximum energy product increased upon decreasing the temperature, as can be seen in Fig. 4.

The maximum energy product $(BH)_{\text{max}}$ at room temperature and at 4.2 K is found to increase with increasing the Hf concentration reaching a maximum value (at room temperature) of 3.7 MGOe for $x = 4$ then it decreases with increasing x , as can be

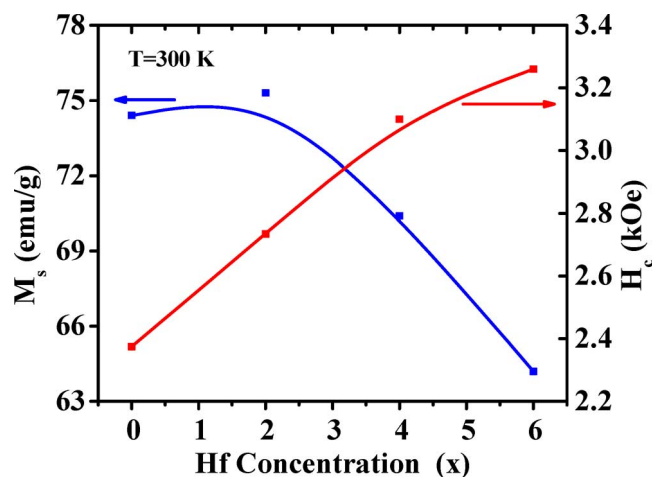


Fig. 3. Dependence of the room temperature saturation magnetization and the coercivity on the Hf concentration for the nanocrystalline ribbons system $Zr_{18-x}Hf_xCo_{82}$.

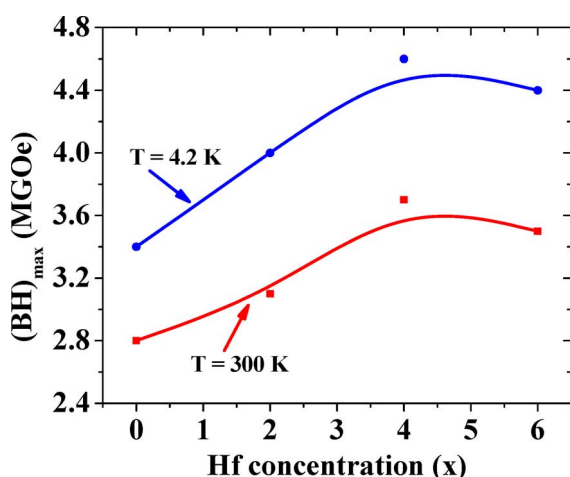


Fig. 4. Dependence of the maximum energy product $(BH)_{max}$ at room temperature and at 4.2 K on the Hf concentration for the nanocrystalline ribbons system $Zr_{18-x}Hf_xCo_{82}$.

seen in Fig. 4. The increase in the energy product with x arises from the improvement of coercive force and rectangular of hysteresis loops due to the refinement of the structure. The magnetocrystalline anisotropy parameter K was calculated to be 1.1 MJ/m^3 for $x = 0$ and 6 , which shows the independence on Hf content.

Fig. 5 shows the Transmission Electron Microscopy images (TEM) for two representative samples of the nanocrystalline ribbons system $Zr_{18-x}Hf_xCo_{82}$ with $x = 0$ and $x = 6$. The energy dispersive X-ray analysis has been used to discern the grain composition. The large grain represents the hard magnetic phase. Its mean size is almost unchanged with the increase of Hf content. The small grain corresponds to soft magnetic phase such as Co indicated by white crosses. It is evident that the average grain size of the soft phase decreases with the increase in Hf concentration. The area of soft phase decreases with the increase of Hf content, implying that the volume fraction of soft phase decreases. The above results are in good agreement with the XRD results.

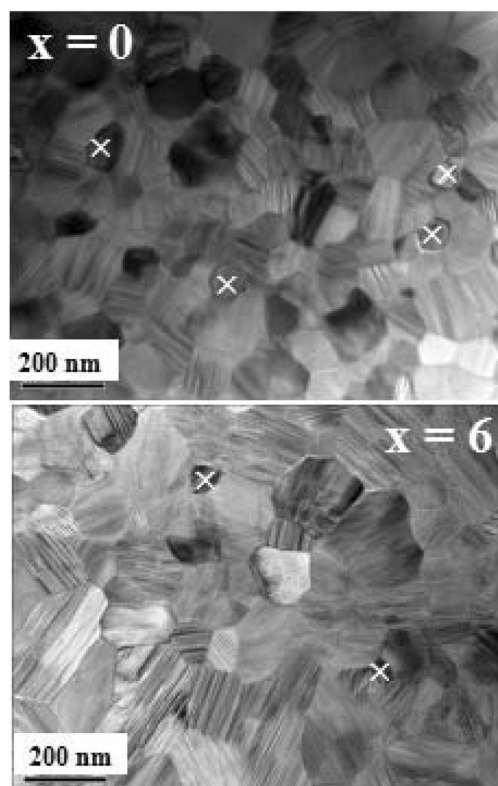


Fig. 5. TEM images for two representative samples of the nanocrystalline ribbons system $Zr_{18-x}Hf_xCo_{82}$ ($x = 0$ and 6).

IV. CONCLUSION

We have investigated the magnetic and structural properties of nanocrystalline rapidly solidified $Zr_{18-x}Hf_xCo_{82}$ ribbons. Structural studies revealed the formation of four phases: rhombohedral Zr_2Co_{11} , orthorhombic Zr_2Co_{11} , hcp Co, and cubic Zr_6Co_{23} phases. Magnetic measurement results showed that all the samples have ferromagnetic behavior at room temperature. The saturation magnetization and the coercivity are found to depend on the Hf concentration at room temperature and at low temperature, 4.2 K. The maximum energy product $(BH)_{max}$ at room temperature was found to increase with increasing the hafnium concentration reaching a maximum value of 3.7 MGOe for $x = 4$, then it decreases as x increases. The magnetocrystalline anisotropy parameter K calculated and was found to be 1.1 MJ/m^3 for $x = 0$ and 6 , which shows the independence on Hf content. The above results indicate the improvement of the energy product of the rare-earth-free high Curie temperature permanent-magnet ribbons upon the Hf addition which was attributed to the refinement of the structure.

ACKNOWLEDGMENT

The authors are grateful to the support from DOE/Ames/BREM under Grant DE-AC02-07CH11358. One author, Al-Omari acknowledges Sultan Qaboos University for the support provided in this study under Grant IG/SCI/PHYS/12/02.

REFERENCES

- [1] E. Burzo, R. Grössinger, P. Hundegger, H. R. Kirchmayr, R. Krewenka, O. Mayerhofer, and R. Lemaire, "Magnetic properties of $ZrCo_{5.1-x}Fe_x$ alloys," *J. Appl. Phys.*, vol. 70, p. 6550, 1991.

- [2] T. Saito, "High performance Co-Zr-B melt-spun ribbons," *Appl. Phys. Lett.*, vol. 82, p. 2305, 2003.
- [3] T. Ishikawa and K. Ohmori, "Hard magnetic phase in rapidly quenched Zr-Co-B alloys," *IEEE Trans. Magn.*, vol. 26, p. 1370, 1990.
- [4] J.-B. Zhang, Q.-W. Sun, W.-Q. Wang, and F. Su, "Effects of Mo additive on structure and magnetic properties of $\text{Co}_{82}\text{Zr}_{18}$ alloy," *J. Alloys and Comp.*, vol. 474, p. 48, 2009.
- [5] G. Stroink, Z. M. Stadnik, G. Veau, and R. A. Dunlap, "The influence of quenching rate on the magnetic properties of microcrystalline alloys $\text{Co}_{80}\text{Zr}_{20-x}\text{B}_x$," *J. Appl. Phys.*, vol. 67, p. 4963, 1990.
- [6] C. Gao, H. Wan, and G. C. Hadjipanayis, "High coercivity in non-rare-earth containing alloys," *J. Appl. Phys.*, vol. 67, p. 4980, 1990.
- [7] L. Y. Chen, H. W. Chang, C. H. Chiu, C. W. Chang, and W. C. Chang, "Magnetic properties, phase evolution, and coercivity mechanism of $\text{Co}_x\text{Zr}_{98-x}\text{B}_2$ ($x = 74-86$) nanocomposites," *J. Appl. Phys.*, vol. 97, p. 10F307, 2005.
- [8] H. H. Stadelmaier, T. S. Jang, and E.-Th. Henig, "What is responsible for the magnetic hardness in Co-Zr(B) alloys?," *Matter. Letter.*, vol. 12, p. 295, 1991.
- [9] M.-Y. Zhang, J.-B. Zhang, C.-J. Wu, W.-Q. Wang, and F. Su, "Hard magnetic properties in melt-spun $\text{Co}_{80}\text{Zr}_{18-x}\text{Mo}_x\text{B}_2$ alloys," *Physica B*, vol. 405, p. 1725, 2010.
- [10] L. Pareti, M. Solzia, and A. Paoluzi, "Magnetocrystalline anisotropy of the 3d sublattice in the cubic intermetallic system $\text{Zr}_6\text{Co}_{23-x}\text{M}_x$ ($\text{M}=\text{Fe}, \text{Ni}$)," *J. Appl. Phys.*, vol. 73, p. 2941, 1993.
- [11] W. Zhang, S. R. Valloppilly, X. Li, R. Skomski, J. E. Shield, and D. J. Sellmyer, "Coercivity enhancement in $\text{Zr}_2\text{-Co}_{11}$ based nanocrystalline materials due to Mo addition," *IEEE Trans. Magn.*, vol. 48, p. 3603, 2012.
- [12] D. Okai, R. Nagai, G. Motoyama, T. Fukami, T. Yamasaki, Y. Yokoyama, H. M. Kimura, and A. Inoue, "Superconducting property of Zr-Co and Zr-Co-Al alloys fabricated by rapid solidification," *Physica C*, vol. 470, p. 1048, 2010.
- [13] B. Balamurugan, B. Das, V. R. Shah, R. Skomski, X. Z. Li, and D. J. Sellmyer, "Assembly of uniaxially aligned rare-earth-free nanomagnets," *Appl. Phys. Lett.*, vol. 101, p. 122407, 2012.
- [14] B. Balamurugan *et al.*, "Magnetism of dilute Co(Hf) and Co(Pt) nanoclusters," *J. Appl. Phys.*, vol. 111, p. 07B532, 2012.
- [15] G. C. Hadjipanayis, D. J. Sellmyer, and B. Brandt, "Rare-earth-rich metallic glasses. I. Magnetic hysteresis," *Phys. Rev. B*, vol. 23, p. 3349, 1981.